Improving sensitivity of gold nanoparticles-based lateral flow assays by using wax-printed pillars as delay barriers of microfluidics

Lourdes Rivas[a,b], Mariana Medina-Sánchez[a], Alfredo de la Escosura-Muñiz[a] and Arben Merkoçi*[a,c]

[a]ICN2 – Nanobioelectronics & Biosensors Group, Institut Catala de Nanociencia i Nanotecnologia, Campus UAB, 08193 Bellaterra (Barcelona), Spain

[b]Departament de Química, Universitat Autònoma de Barcelona, 08193, Bellaterra (Barcelona), Spain

[c]ICREA – Institucio Catalana de Recerca i Estudis Avançats, 08010 Barcelona, Spain

*Corresponding author: arben.merkoci@icn.cat Tel: +34937374604

ABSTRACT

Although lateral flow assays (LFA) are currently being used in some point-of-care applications (POC) they cannot still be extended to a broader range of analytes for which higher sensitivities and lower detection limits are required. To overcome such drawbacks, we propose here a simple and facile alternative based on the use of delay hydrophobic barriers fabricated by wax-printing so as to improve the LFA sensitivity. Several wax pillars patterns were printed onto nitrocellulose membrane in order to produce delays as well as pseudo turbulences into the microcapillary flow. The effect of the proposed wax pillar modified devices were also mathematically simulated corroborating the experimental results obtained for the different patterns tested afterwards for detection of HIgG as model protein in a gold nanoparticle-based LFA. The effect of the introduction of such wax-printed pillars was the sensitivity improvement of almost 3-folds in comparison to a conventional free-barrier LFA.

INTRODUCTION

Constituted mainly by cellulose fibers, paper results very attractive for fabricating biosensors because of its low cost, flexibility and light weight making it useful for transport and storage. In addition, it has the capability to wick liquids via capillary action without use of external pumps and its biocompatibility makes it suitable for immobilizing biomolecules *e.g.* proteins.[1]

Paper has gained much interest in fabrication of diagnostic devices due to the necessity to use low cost materials for a single use, simplifying the fabrication process. Paper-based microfluidic is an emerging technology which uses the paper as substrate creating complex patterns of hydrophilic channels and hydrophobic barriers by using patterning techniques such as: photolithography,[2] wax patterning,[3,4] inkjet etching,[5] flexographic printing[6] and screen printing.[7]

The first paper-based sensor can be considered the paper chromatography developed by Martin and Synge at the beginning of 1940's.[8] Fifteen years later, the first semiquantitative paper-based biosensor for detection of glucose in urine,[9] became the commonest commercially available point-of-care (POC) lateral flow assay (LFA) device. Initially, the main application of LFAs was a pregnancy test[10] while nowadays their applications is extended to a wide variety of analytes that include cancer biomarkers,[11,12] DNA,[13,14] toxins[15,16] and metals.[17,18]

LFAs are characterized by their simple use, rapid result, low cost, good specificity and long shelf life. However, they suffer analytical performance limitations, mainly due to sensitivity and reproducibility issues. In this context, many efforts have been developed in order to improve the LFA sensitivity using different alternatives as immuno-gold silver staining,[19] dual gold nanoparticle (AuNP) conjugates[20] and AuNP loaded with

enzymes[21]. Beside AuNPs other labels such as fluorescent Eu(III) nanoparticles[22] and quantum dots[23] have been also reported. Changes on the paper architecture were also proposed for improving the performance of LFA.[24]

The most important part of a LFA is the detection membrane which is made of cellulose nitrate or nitrocellulose (NC), a porous material where the capture reagents (*e.g.* antibodies) are immobilized due to a possible combination of electrostatic and hydrophobic forces.[25] In fact, NC has been widely used in blotting techniques thanks to its capacity of interact with proteins, DNA and RNA.[26] Wax printing is a simple and low cost patterning technique based on the melting of solid wax printed onto porous substrate, which has been used for fabricating paper-based microfluidics in NC membrane and its application in protein pattern and dot immunoassay.[4] Recent reports have demonstrated the possibility to control the reagent transport by using novel and sensitive methods such as dissolvable barriers[27,28] and bridges made of sugars,[29] fluidic diodes and valves[30] and tunable-delay shunts.[31] Despite of their capability to improve the performance of paper-based devices which is related with their sensitivity, some of these methods are time consuming and require more reagents for fabricating of the devices.

We present here a new strategy for improving the sensitivity of gold nanoparticle-based lateral flow assays by using barriers (pillars) deposited onto the nitrocellulose membrane by wax printing technique. Different pillar designs were printed, in order to create hydrophobic barriers that can cause flow delay. To check the efficiency of such pillars, we used membranes with relatively fast flow so as to obtain higher sensitivity and low detection limits. The controlled delays in microfluidics increase the binding time between the immunocomplex and the detection antibody, in addition to the

generation of pseudo turbulences in the pillars zone that improves mixing between the analyte and the labeled antibody. This microfluidics delay in certain zones (incubation areas) combined with the generation of the pseudo turbulences directly affects the analytical performance of the LFA being transduced to a better sensitivity and detection limit.

MATERIALS AND METHODS

Chemicals and equipment

Hydrogen tetrachloroaurate (III) trihydrate ($HAuCl_4 \cdot 3H_2O$, 99.9%), trisodium citrate ($Na_3C_6H_5O_7 \cdot 2H_2O$), phosphate buffer saline tablet (P4417), human IgG from human serum (I2511), anti-human IgG (polyclonal antibody developed in goat; I1886) and anti-human IgG γ-chain specific-biotin (polyclonal antibody developed in goat; B1140) were purchased from Sigma-Aldrich (Spain). Anti-goat IgG (polyclonal antibody produced in chicken; ab86245) was purchased from Abcam (UK).

All the materials used for the production of the LFIA strips were purchased from Millipore (Billerica, USA): sample and absorbent pads (CFSP001700), conjugate pad (GFCP00080000), detection pads (Hi-Flow Plus 75, SHF0750425 and Hi-Flow Plus 75, SHF2400425) and the backing card (HF000MC100). mQ water, produced using a Milli-Q system (>18.2 MΩ cm^{-1}) purchased from Millipore was used for the preparation of all solutions. A thermostatic centrifuge (Sigma 2-16 PK, Fisher Bioblock Scientific, France) was used to purify the AuNP/antibody conjugates. A Xerox ColorQube 8570 wax printer (Xerox Corporation, USA) was used for printing different wax designs. A hot plate (VWR, USA) was used for heating and melting the wax ink. An IsoFlow reagent dispensing system (Imagene Technology, USA) was used to dispense the

detection and control lines. A guillotine (Dahle 533, Germany) was used to cut the strips. The stirrer used was a TS-100 Thermo shaker (BioSan, Latvia). A strip reader (COZART — SpinReact, UK) was used for quantitative measurements. All the size measurements and shape observation of AuNPs were conducted in a Field Emission Gun Transmission Electronic Microscope Fei, model Tecnai^{TM} G2F20 (Fei, USA). A spectrophotometer SpectraMax M2^{e} (Molecular Devices, UK) was used to record all UV-Vis spectra of AuNPs. Scanning electronic micrographs of nitrocellulose membrane were conducted in a Field Emission Gun Scanning Electronic Microscope Fei, model Quanta^{TM} 650 (Fei, USA). A Leica DCM 3D dual core 3D measuring microscope (Leica Microsystems, Germany) was used for confocal images of nitrocellulose membrane. An image processing software, ImageJ (National Institute of Health, USA) was used for measuring the size of the wax pillars before and after melting step.

Preparation of gold nanoparticles (AuNPs)

Gold nanoparticles (AuNPs) 20 nm sized and stabilized by citrate, were prepared using the Turkevich's method.[32] Briefly, 50 mL aqueous solution of 0.1% $HAuCl_4$ was heated to boiling and vigorously stirred in a 250 mL round-bottom flask; 1.25 mL of sodium citrate 1% were added quickly to this solution. Boiling was continued for additional 10 min. The solution was cooled to room temperature with a continuous stirring. The colloids were stored in dark bottles at 4° C. All glassware used in this preparation was previously cleaned in *aqua regia* overnight and rinsed with double distilled H_2O and reflux was used for all the procedure.

AuNPs modification with antibodies

AuNPs were modified with antibodies following a previously optimized procedure.[33] First, the pH of the AuNPs suspension was adjusted to pH 9 with 0.1 M borate buffer. Then, 100 µL of a 100 µg mL^{-1} anti-human IgG γ-chain specific-biotin aqueous solution were added to 1.5 mL of the AuNPs suspension. The resulting solution was incubated for 20 min at 650 rpm. Then, 100 µL of 1 mg mL^{-1} BSA aqueous solution were added and the stirring was continued for other 20 min at 650 rpm. Finally, the solution was centrifuged at 14000 rpm and 4ºC for 20 min.

The supernatant was removed and the pellet of AuNP/anti-Human IgG was re-suspended in 500 µL of BB 2 mM pH 7.4, 10% sucrose.

Preparation of the strips

Once the pillar patterns have been designed with graphic design software (Corel Draw X4), the preparation of the modified detection pad consisted in three main steps: i) printing the pillars patterns onto the nitrocellulose (NC) membrane (Hi-Flow Plus 75, HF075) with a wax printer; ii) heating the NC membrane and melting the wax at 110ºC for 90 seconds by using the hot plate; and iii) dispensing antibodies onto the membrane. For this step, 1 mg mL^{-1} solution of anti-Human IgG (whole molecule) and anti-Goat IgG were spotted onto the detection pad at dispensing rate of 0.05 µL mm^{-1} using an IsoFlow reagent dispensing system so as to form the test and control line, respectively. Then, the detection pad was dried at 37ºC for 1 h.

The sample pad was prepared by dipping into 10 mM PBS, 5% BSA and 0.05% Tween®-20 and drying at 60ºC for 2h. The conjugate pad was prepared dipping it into the previously prepared anti-Human IgG γ-chain specific-biotin/AuNP conjugate and drying under vacuum for 1 h.

The different pads were sequentially laminated 2 mm with each other and pasted onto the adhesive backing card in the following order: detection, conjugation, sample and absorbent pads. Finally, the strips were cut 7 mm wide and used immediately.

Lateral-flow assay procedure

Sample solutions of 200 µL of different concentration Human IgG (HIgG) in PBS 10 mM, pH 7.4, ranging from 5 ng mL^{-1} to 500 ng mL^{-1} were dispensed onto the sample pad and keeping for 15 min until the flow is stopped. Then 200 µL of PBS was dispensed in order to wash away the excess of AuNPs/antibody. After drying the lateral flow strips at room temperature, they were read with the strip reader so as to obtain the calibration curve for HIgG. PBS without analyte was considered as blank. All the measurements were carried out by triplicate.

Mathematical simulations

Flow in porous media can be studied by the use of the Navier-Stokes equations, which describe the movement of fluid substances, which represent the effect of the diffusing viscosity and the pressure. These equations coupled with the Brinkman equations, can be useful for modeling of the flows through certain porous media. The initial conditions for the simulation such as porosity and permeability of the membranes (in this case, a different kind of membrane was used) were the same as in a previous work reported in our group.[24] These parameters were given by Millipore Corporation (porosity around 83%, and the permeability $4.3x10^{-6}$ m^2). On the other hand, the density and viscosity values at 25ºC (0.997 g mL^{-1} and 0.890 N s m^{-2}) used were the ones of the water as an approximation. The boundary conditions for the simulation were the geometry (changing the pillars distribution). The velocity was calculated from the volume of the

liquid introduced into the membrane (200 µL) and the cross section area of the absorbent pad and the time necessary to absorb the respective volume (1.47 m s^{-1}).

RESULTS AND DISCUSSION

Improvement of sensitivity of lateral flow assay by using wax delay barriers

Lateral flow assays must allow rapid responses with good sensitivity. For this purpose, manufacturers have developed different membranes which satisfy these requirements. Capillary flow rate is a common parameter to classify the membranes on basis of the required time for the liquid to travel and fill completely a 4-cm length of membrane. In this work, nitrocellulose membranes Hi-Flow Plus 75 (HF075) and Hi-Flow Plus 240 (HF240) provided by Millipore Corporation were used. The first one has a nominal flow rate of 75 s across 4 cm of membrane, and the last one has a higher nominal flow rate of 240 seconds across the same length.[34] Sensitivity in LFA is conditioned by various factors being crucial the performance of nitrocellulose membrane.

For a fast liquid velocity membrane (HF075), the sensitivity is low due to two main factors: i) the liquid takes less time to travel a defined length and ii) the formation of the immunocomplex between the analyte and AuNP-labeled antibody at the conjugate pad, as well at test and control lines, is less effective since the flow rate is faster. In the case of a slow velocity membrane (HF240) the sensitivity is higher since the flow rate is slower and there is enough time for an effective formation of immunocomplex at the beginning of the strip and at test and control line.

Based on that, we chose the faster membrane provided by Millipore (HF075) for its modification with wax pillars using the wax-printing technology so as to evaluate the effect (in terms of sensitivity and limit of detection) produced by these hydrophobic

structures that can act as obstacles for delaying the sample flow on a AuNP-based LFA (see Fig. 1).

Wax printing technology is used here to deposit wax on the surface of nitrocellulose, followed by a heating step for melting the wax pattern for its penetration through the pores of the membrane while maintaining the original design. The hydrophobic properties of the wax, make it suitable for the creation of barriers which can modulate the flow on membranes in a desirable way, *e.g.* for controlling the delivery time of reagents.[35]

In the wax printing process, the nitrocellulose membrane to be printed passes between the pressure roller and the print drum of the printer, suffering changes due to the pressure. To evaluate these alterations, empirical calculations of permeability and scanning electron micrographs for membranes characterizations were carried out.

In figure 2 transversal cuts of membranes with and without modifications produced just by applying heat and pressure are shown. When the membrane passes through the wax printer, a thickness reduction of around 30 μm is observed due to the compression produced by the pressure roller and the drum of the printer (figure 2A-B). The results of the LFA performed for both approaches (figures 2C-2D) were compared so as to estimate the effect of mechanical compression of membrane in quantitative measurements (HIgG concentrations: 5, 50 and 500 ng mL^{-1}). Indeed, when the membrane is flattened the sensitivity of LFA increases due to the fact that the modified membrane became thinner and this compression produces wider reagent lines making them easier to visualize a weak signal. This is related to the fact that due to the spreading of reagents, the fluid afterwards penetrates the whole thickness of the membrane laterally moving producing wider lines due to less depth to contain the same

volume of reagent.[34] The limit of detection (LoD) using the strip reader (for all the LF formats described) was calculated as the concentration of HIgG corresponding to three times the standard deviation of the estimate, giving a value for the LF strips (with flattened membranes HF075) of 8.0 ng mL^{-1} of HIgG while by using membranes without any modification, this value is of 12 ng mL^{-1}. This suggests that only the compression of nitrocellulose membranes gives a 1.5-fold improvement in the sensitivity of the assay.

In traditional printing methods, the porosity plays an important role on the absorption of the ink by different paper substrates: high porosity papers absorb and spread more ink, while low porosity papers can prevent the penetration of the ink through their fibers. In the wax printing process used in this work, the wax penetrates only into superficial fibers of nitrocellulose. To ensure the presence of delay barriers along the whole thickness of the membrane, a melting process was conducted. Two nominal wax pillars of 0.4 and 1.0 mm diameters were measured before and after melting process, and results showed that wax pillar diameters increased up to 20% regarding to the original printing size after melting step (see Figure S1). Once the melted wax enters through the fibers of membrane a lateral spreading occurs and decreases the resolution of the printed pattern, which is affected by the porosity and thickness of membrane.[3] Although just one type of NC membrane was employed for printing purposes (approximate pore size 12-17 µm), if a membrane with smaller pores is used, the increment after melting could be lower due to the higher packaging of nitrocellulose fibers that reduces the possibility of air passages and avoids the spread of the ink. The effect on the sensitivity caused by changing the wax pillar diameter was tested in quantitative measurements of HIgG. Results showed that the presence of wax pillars with small diameters (0.4 mm) reduced considerably the unspecific signals, showing strips with clear backgrounds and a better

differentiation of intensities of test lines observed through the concentration range if compared with the modified membrane (see Figure S2 A-B). Regarding to the sensitivity, the presence of small diameter wax pillars produces a slight increment of 1.2-fold respect to the modified membrane, which corresponds to a LoD of 6.6 ng mL^{-1}. This result indicates that wax pillars are acting as delay barriers of the fluid due to their hydrophobic nature allowing in this way, a suitable recognition between the analyte and the capture AuNP labeled antibody before arriving to test line. However, this size (0.4 mm) was not enough to increase even more the sensitivity of the assay. On the other hand, wax pillar of a bigger diameter (1.0 mm) was tested and experimental results showed that sensitivity was affected. This occurred because the pillars delayed the regular flow in such way that the time of the assay was substantially long making it useless for practical purposes; a considerable amount of AuNPs which could not reach properly to test and control lines remained along the membrane, showing a pink background; thus a high LoD of 15.6 ng mL^{-1} was obtained (see Figure S2-C). It is worthy to note that the wax pillar size is an important parameter that affects the sensitivity in different ways and the proper choice for wax pillar size must be a compromise between the sensitivity and the time of the assay.

For the remaining experiments, the wax pillars diameter chosen was 0.5 mm and the effect produced by different wax pillars arrangements on the microfluidic was tested. Four different patterns (“P1”, “P2”, “P3” and “P4”) as well as strips with and without modifications were tested for HIgG detection. Experimental results clearly showed the effect on the sensitivity of the assay produced by the wax pillars geometries (see Fig. 3). As stated before, an improvement of sensitivity is produced by: i) mechanical compression of membrane and ii) the presence of wax pillars of proper size. Slightly increasing the diameter of the wax pillar up to 0.5 mm, it was possible to improve the

sensitivity, especially for “P1” and “P2” patterns up to 1.7- and 2.6-fold respect to modified and unmodified membrane, respectively. These results showed that sensitivity in LFA can be affected by presence of wax pillars, their diameters and also the spatial arrangements. Moreover, mathematical simulations were performed to study these phenomena. For each pattern, the flow speed, vorticity and force around the pillars, were calculated at the end of the pillars zone and control line. All these data are summarized in Table 1.

Three different flow parameters were mathematically considered to correlate them with the experimental results. Mathematical simulations for HF075 were achieved as blank in order to compare the differences observed in the mentioned parameters in the presence of several wax pillars patterns. According to the data in Table 1, the highest flow velocities at the end of wax pillars zone corresponds to patterns “P1” and “P2” which are compensated by the vorticity range (a physical magnitude that describes the rotation of a fluid near to some point). While bigger is this range, higher is the rotation of the fluid. In addition, the pressures are higher for these two patterns. These results are consistent with the most sensitive modified LFA which are “P1” and “P2” patterns. Making the same considerations for the remaining patterns, the “P3” resulted with higher flow velocities and vorticity values and low pressure compared with “P4”. However, the experimental results showed that LoD for “P4” (6.5 ng mL^{-1}) is better than the obtained for “P3” (8.2 ng mL^{-1}).

With the purpose to confirm if the wax truly acts as a barrier across membrane, characterizations by using scanning electron and confocal microscopes were performed. A transversal cut of wax dots area in order to verify if the melted wax penetrates through the entire thickness of membrane was made as it is shown in figure 4A. Due to

the density of the wax and membrane itself, it was difficult to characterize by SEM if the area of barriers was only covered with wax. Therefore it was necessary to characterize the area of barriers by using confocal technology. Figure 4B shows a surface roughness profile on the wax dots area and it is possible to observe different surface roughness values. This means that the melted wax (darker points) has filled the pores of the membrane creating a tridimensional structure (like a pillar) capable of obstructing the normal flow of the sample across the whole membrane thickness (Fig. 4C).

Based on the previous experimental results and mathematical simulations, “P3” and “P4” wax patterns were discarded due to the fact that they showed a lower sensitivity compared to “P1” and “P2” and an accurate calibration curve was carried out (see Figure 5). In this experiment, unmodified and modified membranes (HF075 and HF240), where used to compare the effect produced by mechanical compression and also, the presence of the wax pillars on LFA. As expected, unmodified HF075 membrane presents less sensitivity as its capillary flow time is lower if compared with unmodified HF240 membrane. This means that sample flow needs shorter time interval to travel a defined distance on the membrane, thus there is not enough time for formation of the immunocomplex and its sensitivity is affected.

When the HF075 membrane suffered the mechanical compression by the roller and the print drum, detection lines became wider and its sensitivity increased as stated before. LoD for modified HF075 membrane is comparable to the value obtained for the most sensitive unmodified membrane HF240. In addition, the selected patterns showed lower LoD regarding to the value obtained for the most sensitive membrane, HF240, produced by Millipore. The reproducibility of the responses (n=3) for a 100 ng mL^{-1} HIgG

concentration was also studied, and relative standard deviation (RSD) and limits of detection for different patterns and membranes can be found in the ESI.

Lateral flow assays with printed wax pillars resulted to be more sensitive and showed lower limits of detection than lateral flow assays without modifications. Moreover, all blank measurements gave a lower background signal compared with LFA without modifications.

In order to verify which is the role of the location of wax pillars patterns in the sensitivity of LFA, two "P2" patterns have been studied: one near to the conjugate pad (P2a) and other one near to the test line (P2b). Results showed that there is not any significant difference on the value of the limit of detection if the wax pattern is located near or far away from the conjugate pad. This is attributable to the fact that the capillary flow rate is considerably faster at the beginning of the detection membrane and decreases exponentially as the liquid moves along it, until reaching a steady flow rate when the bed volume of membrane is saturated.[34] Therefore, when the wax pillars area is located at the beginning of the membrane this is enough to improve the sensitivity of LFA. In addition this contributes significantly to delay the flow rate leading to better limits of detection.

Wax printing was used as patterning technique, in order to create delay barriers on LF devices that lead to increase on sensitivity of the assays. Despite of the sensitivity improvements obtained by the developed devices, these are fast, easy to use, low-cost and their fabrication just includes an extra step of printing that takes few minutes, compared with other controlling fluid methods previously reported, which are more sensitive but the fabrication are laborious and require additional reagents.

In this context, our approach constitutes an important strategy for the sensitivity improvement on lateral flow assays using paper-based microfluidic techniques, that can be improved by other techniques such as inkjet technology, which allows to print directly on the surface of nitrocellulose membrane by using a hydrophobic solution or ink capable to create well defined patterns without have direct contact with it.[36]

CONCLUSION

We have presented a new and easy strategy for improving the sensitivity of a gold nanoparticle-based LFA by the deposition of hydrophobic barriers of wax printed at the detection pad of a LFA. These barriers act as obstacles delaying the regular flow on the strip by increasing the binding time between the analyte and the labeled antibody and therefore allowing an effective formation of immunocomplex. Different designs were evaluated and the optimized ones allowed improving of almost 3-folds the limit of detection compared with the non-modified membranes. Mathematical simulations corroborate the experimental results obtained for the different patterns. This approach is simpler than other previously reported strategies since is not time-consuming, is low-cost, does not require the use of additional reagents for signal amplification or even changes on the configuration of LF strip. In consequence, the proposed strategy can be easily extended to any type of LFA design and could expand the landscape to the use of LF designs with patterning techniques facilitating its use in point-of-care applications.

ACKNOWLEDGMENTS

We acknowledge MINECO (Madrid) for the project MAT2011-25870. L.R. also acknowledges *Universitat Autònoma de Barcelona* for her pre-doctoral grant.

REFERENCES

1. C. Parolo and A. Merkoçi, *Chem. Soc. Rev.*, 2013, **42**, 450–457.

2. A. W. Martinez, S. T. Phillips, M. J. Butte, and G. M. Whitesides, *Angew. Chem. Int. Ed. Engl.*, 2007, **46**, 1318–1320.

3. E. Carrilho, A. W. Martinez, and G. M. Whitesides, *Anal. Chem.*, 2009, **81**, 7091–7095.

4. Y. Lu, W. Shi, J. Qin, and B. Lin, *Anal. Chem.*, 2010, **82**, 329–335.

5. K. Abe, K. Suzuki, and D. Citterio, *Anal. Chem.*, 2008, **80**, 6928–6834.

6. J. Olkkonen, K. Lehtinen, and T. Erho, *Anal. Chem.*, 2010, **82**, 10246–10250.

7. W. Dungchai, O. Chailapakul, and C. S. Henry, *Analyst*, 2011, **136**, 77–82.

8. A. J. P. Martin and R. L. M. Synge, *Biochem. J.*, 1941, **35**, 1358–1368.

9. J. Comer, *Anal. Chem.*, 1956, **28**, 1748–1750.

10. M. C. Brucker and N. J. MacMullen, *J. Obstet. Gynecol. neonatal Nurs.*, 1985, **14**, 353–359.

11. C. Fernández-Sánchez, C. J. McNeil, K. Rawson, and O. Nilsson, *Anal. Chem.*, 2004, **76**, 5649–5656.

12. C. Fernández-Sánchez, C. J. McNeil, K. Rawson, O. Nilsson, H. Y. Leung, and V. Gnanapragasam, *J. Immunol. Methods*, 2005, **307**, 1–12.

13. J. Aveyard, M. Mehrabi, A. Cossins, H. Braven, and R. Wilson, *Chem. Commun.*, 2007, 4251–4253.

14. P. Lie, J. Liu, Z. Fang, B. Dun, and L. Zeng, *Chem. Commun.*, 2012, **48**, 236–238.

15. V. M. T. Lattanzio, N. Nivarlet, V. Lippolis, S. Della Gatta, A. C. Huet, P. Delahaut, B. Granier, and A. Visconti, *Anal. Chim. Acta*, 2012, **718**, 99–108.

16. L. Anfossi, C. Baggiani, C. Giovannoli, G. D'Arco, and G. Giraudi, *Anal. Bioanal. Chem.*, 2013, **405**, 467–480.

17. J. Liu, D. Mazumdar, and Y. Lu, *Angew. Chemie*, 2006, **118**, 8123–8127.

18. A. M. López Marzo, J. Pons, D. A. Blake, and A. Merkoçi, *Anal. Chem.*, 2013, **85**, 3532–3528.

19. I. H. Cho, S. M. Seo, E. H. Paek, and S. H. Paek, *J. Chromatogr. B Anal. Technol. Biomed. Life Sci.*, 2010, **878**, 271–277.

20. D. H. Choi, S. K. Lee, Y. K. Oh, B. W. Bae, S. D. Lee, S. Kim, Y.-B. Shin, and M.-G. Kim, *Biosens. Bioelectron.*, 2010, **25**, 1999–2002.

21. C. Parolo, A. de la Escosura-Muñiz, and A. Merkoçi, *Biosens. Bioelectron.*, 2013, **40**, 412–416.

22. E. Juntunen, T. Myyryläinen, T. Salminen, T. Soukka, and K. Pettersson, *Anal. Biochem.*, 2012, **428**, 31–38.

23. Y.-Y. Lin, J. Wang, G. Liu, H. Wu, C. M. Wai, and Y. Lin, *Biosens. Bioelectron.*, 2008, **23**, 1659–1665.

24. C. Parolo, M. Medina-Sánchez, A. de la Escosura-Muñiz, and A. Merkoçi, *Lab Chip*, 2013, **13**, 386–390.

25. R. C. Wong, *Lateral Flow Immunoassay*, Humana Press, Totowa, NJ, 2009.

26. J. L. Tonkinson and B. A. Stillman, *Front. Biosci.*, 2002, **7**, C1–12.

27. E. Fu, B. Lutz, P. Kauffman, and P. Yager, *Lab Chip*, 2010, **10**, 918–920.

28. B. Lutz, T. Liang, E. Fu, S. Ramachandran, P. Kauffman, and P. Yager, *Lab Chip*, 2013, **13**, 2840–2847.

29. J. Houghtaling, T. Liang, G. Thiessen, and E. Fu, *Anal. Chem.*, 2013, **85**, 11201–11204.

30. H. Chen, J. Cogswell, C. Anagnostopoulos, and M. Faghri, *Lab Chip*, 2012, **12**, 2909–13.

31. B. J. Toley, B. Mckenzie, T. Liang, J. R. Buser, P. Yager, and E. Fu, *Anal. Chem.*, 2013, **85**, 11545–11552.

32. J. Turkevich, P. C. Stevenson, and J. Hillie, *Discuss. Faraday Soc.*, 1951, 55–75.

33. A. Ambrosi, M. T. Castañeda, A. J. Killard, M. R. Smyth, S. Alegret, and A. Merkoçi, *Anal. Chem.*, 2007, **79**, 5232–5240.

34. Millipore Corporation, *Rapid Lateral Flow Test Strips. Considerations for product development*, 2002.

35. H. Noh and S. T. Phillips, *Anal. Chem.*, 2010, **82**, 8071–8078.

36. A. Apilux, Y. Ukita, M. Chikae, O. Chailapakul, and Y. Takamura, *Lab Chip*, 2013, **13**, 126–135.

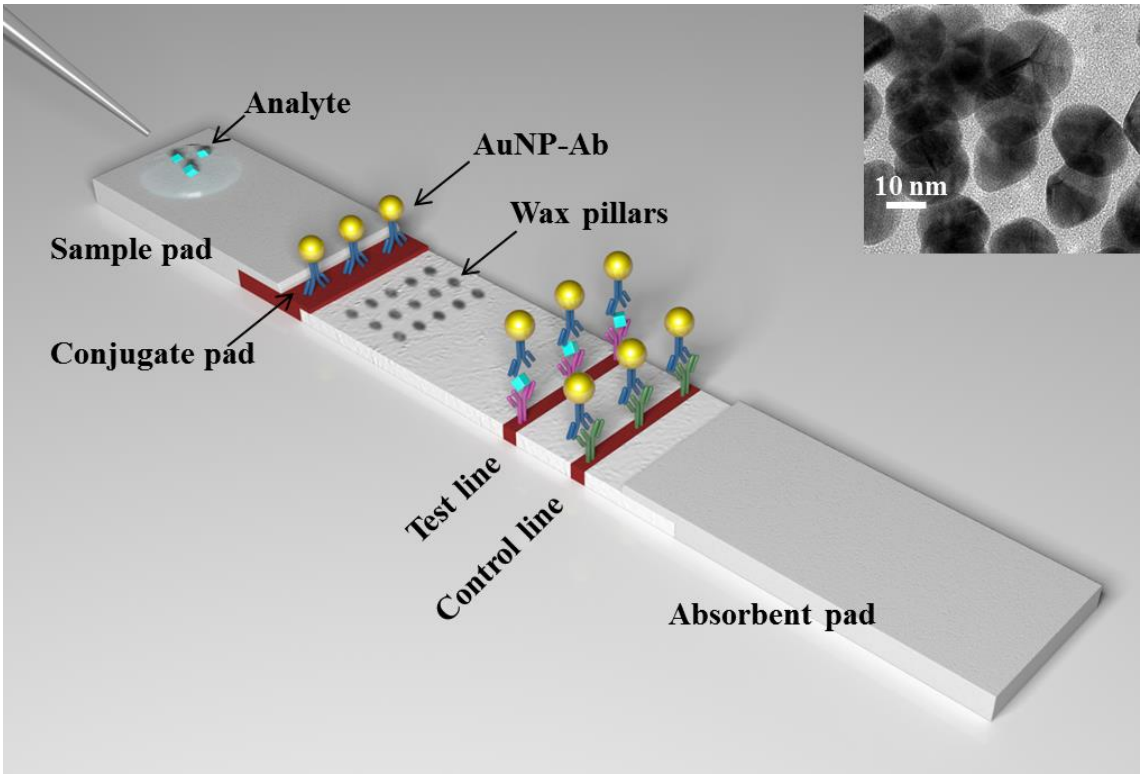

Figure 1. Schematic representation of a lateral flow strip modified with wax pillars for protein detection based on the use of AuNP. (Inset) TEM image of AuNPs used for the lateral flow assay (LFA) development.

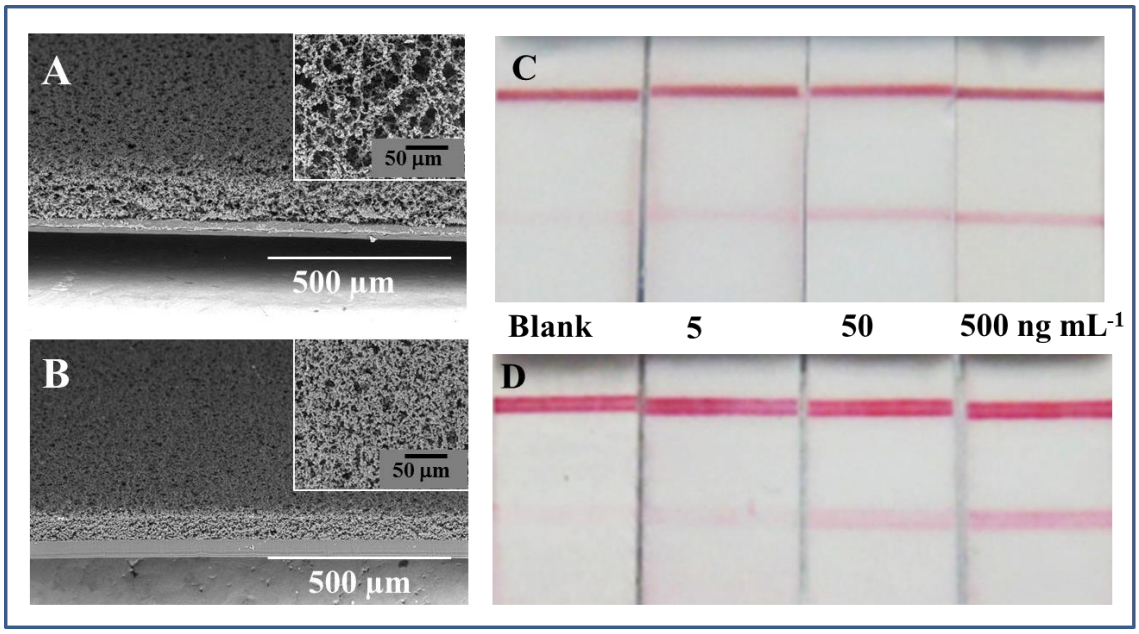

Figure 2. Left: Scanning electron micrographs (SEM) of transversal cuts: (A) unmodified and (B) modified membrane HF075. Right: LFA for HIgG detection using (C) unmodified and (D) heat and pressure-modified membrane for a blank assay and for assays performed with 5, 50 and 500 ng mL^{-1} of HIgG.

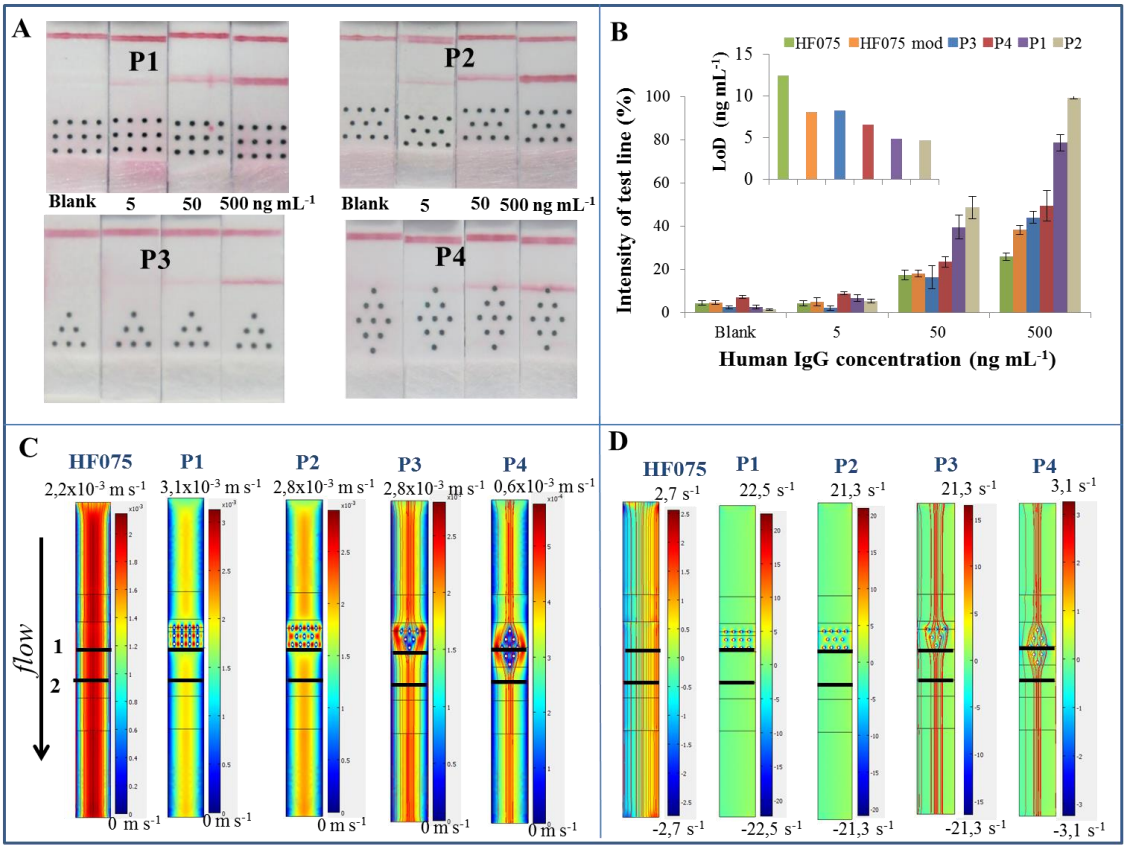

Figure 3. (A) LF strips modified with different pattern of wax pillars. (B) Effect of the wax pillars in LF quantitative measurement for different concentrations of HIgG and the corresponding LoDs (inset). (C) Flow speed simulations for modified and unmodified LF. (D) Simulated results of vorticity for modified and unmodified LF.

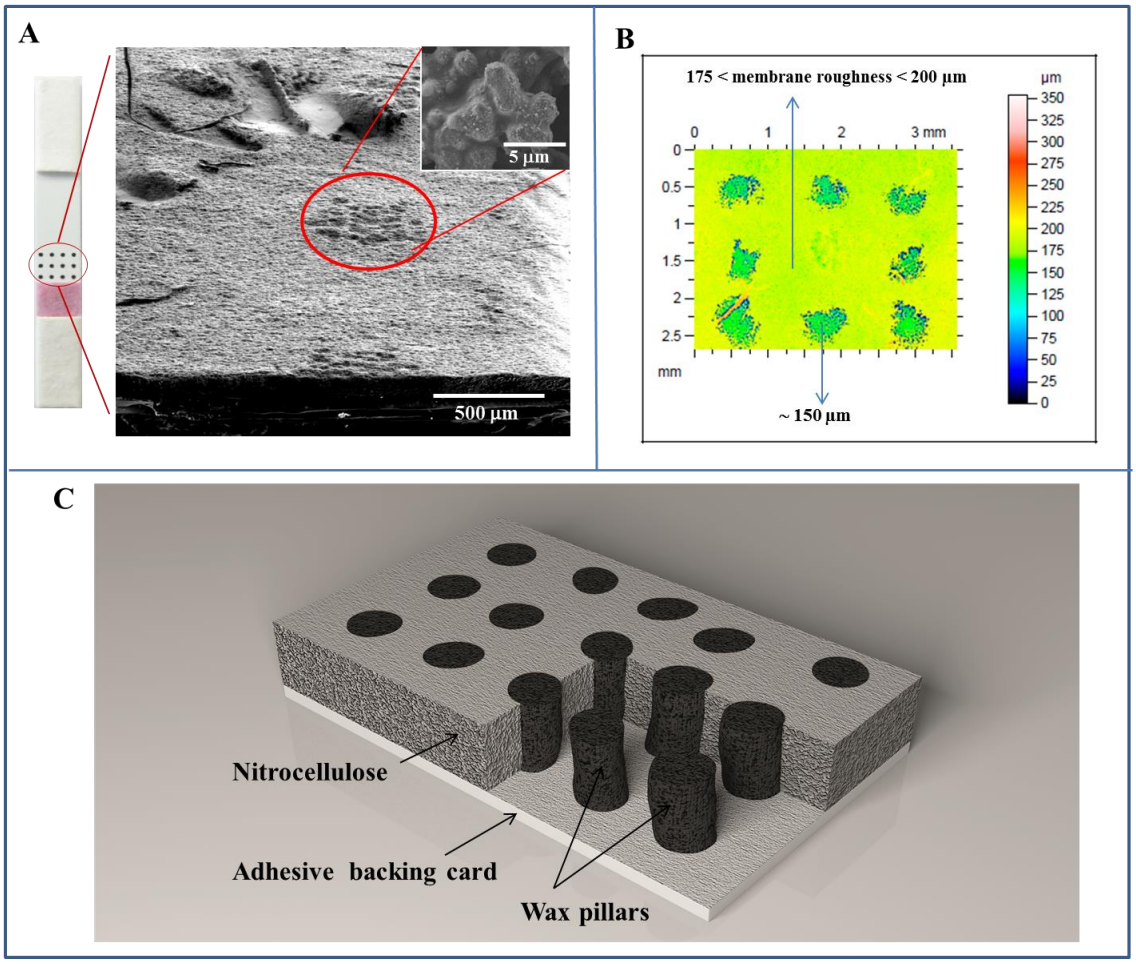

Figure 4. (A) SEM image for transversal cut of wax pillars area on a lateral flow strip. Inset corresponds to a membrane covered with melted wax. (B) Surface profile roughness of LFA modified with wax pillars. (C) Schematic of a transversal cut of pillars zone on nitrocellulose membrane.

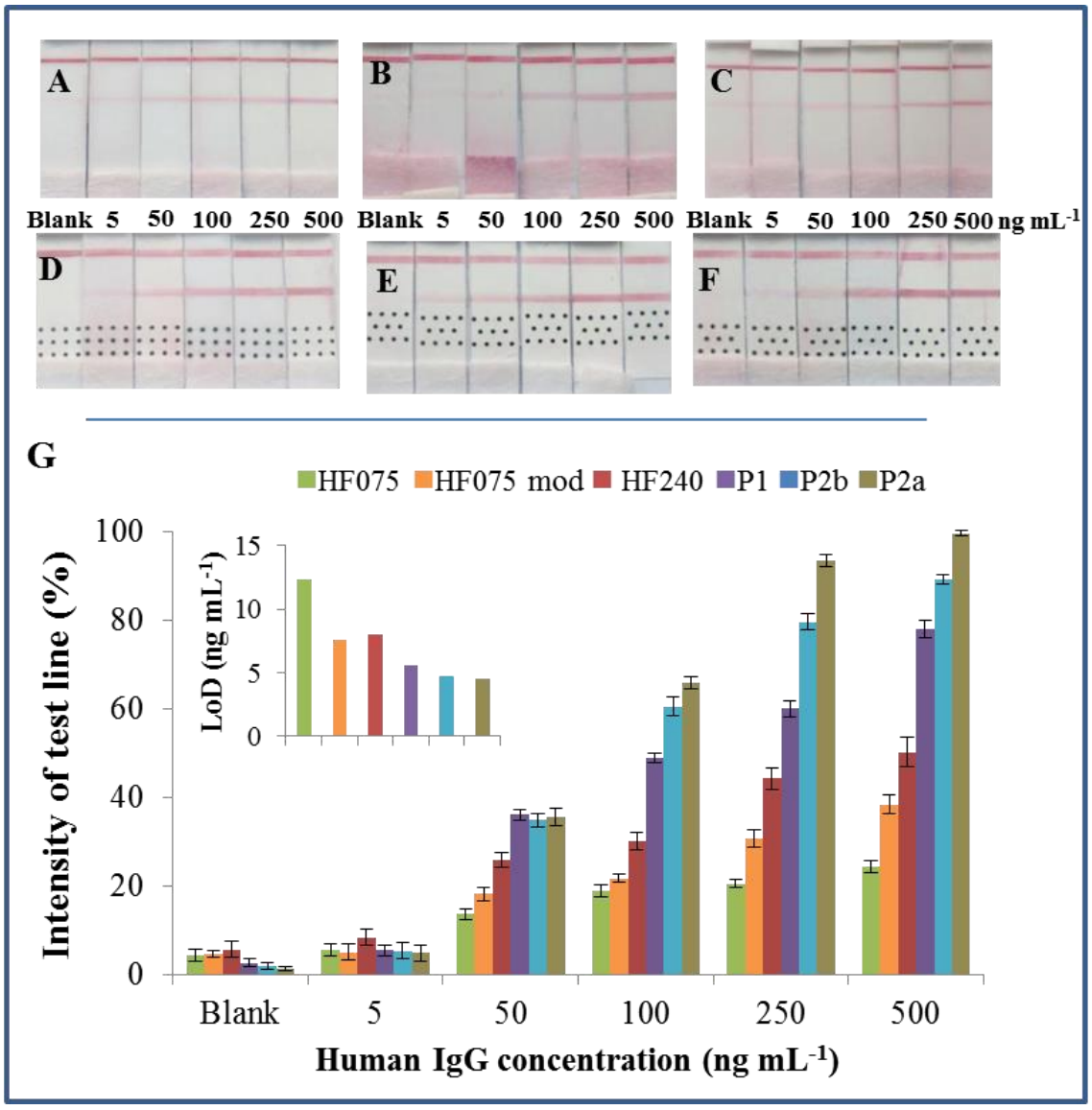

Figure 5. Results of LFA assays for HIgG detection performed with (A) unmodified HF075; (B) modified HF075 and (C) unmodified HF240 membranes. (D), (E), (F) correspond to the same membranes modified with P1, P2b, and P2a patterns, respectively. (G) Quantitative evaluation of the performance of the assays performed with the different membranes.

Table 1. Parameters measured with mathematical simulations for LFAs modified with wax pillars

Pattern	Average Velocity ($x10^{-3}$ m s^{-1})	Vorticity (s^{-1})	Average Pressure Force per unit of area (Pa)
HF075	V_1= 1.03	$Vort_1$= (-1.4 to 1.4)	F_1= 0
	V_2= 1.03	$Vort_2$= (-1.4 to 1.4)	F_2= 0
P1	V_1= 1.60	$Vort_1$= (-4.7 to 4.7)	F_1= 2.5e-5
	V_2= 1.03	$Vort_2$= (-1.4 to 1.4)	F_2= 0
P2	V_1= 1.40	$Vort_1$= (-4.5 to 4.5)	F_1= 2e-5
	V_2= 1.03	$Vort_2$= (-1.4 to 1.4)	F_2= 0
P3	V_1= 1.03	$Vort_1$= (-2.4 to 2.4)	F_1= 3e-8
	V_2= 1.03	$Vort_2$= (-1.4 to 1.4)	F_2= 0
P4	V_1= 0.18	$Vort_1$= (-0.47 to 0.47)	F_1= 3.6e-8
	V_2= 0.18	$Vort_2$= (-0.25 to 0.25)	F_2= 0